Variable Conductance Heat Pipe Radiator for Lunar Fission Power Systems

William G. Anderson[1], Bryan J. Muzyka[2], Christopher J. Peters[3], and John R. Hartenstine[4]
Advanced Cooling Technologies, Inc., Lancaster, PA, 17601, U.S.A.

Ted Stern[5] and Grant Williams[6]
Vanguard Space Technologies, Inc., 9431 Dowdy Dr., San Diego, CA 92126 U.S.A.

Nuclear power systems for long-term Lunar and Martian missions present many challenges to thermal management systems, such as variable thermal loads, large temperature swings between day and night, and freezing of the working fluid. The radiator to reject the waste heat must be sized for the maximum power at the highest sink temperature, but is then oversized for other conditions, such as the Lunar/Martian night, or periods when the power to be rejected is low. A Variable Conductance Heat Pipe (VCHP) radiator can passively accommodate changing thermal loads and environments. A variable conductance thermosyphon radiator was developed and tested, with heat supplied by a single-phase pumped loop. The radiator is designed to operate in the 370 to 400 K temperature range, which is above the operating range of standard aluminum/ammonia radiator panels. To operate at these higher temperatures, the radiator has a titanium heat exchanger, titanium/water thermosyphons, and graphite fiber reinforced composite radiator panels. The radiator is capable of: 1) Accommodating changes in power and sink temperature, 2) Successfully starting up from an initially frozen state with excess water frozen in an arbitrary location, and 3) Shutting down, freezing, and then successfully restarting. A low mass design was developed that accommodates the coefficient of thermal expansion (CTE) mismatch between the titanium heat exchanger and the graphite radiator panel. A full-scale VCHP radiator was fabricated and tested in order to demonstrate functionally at a larger, more representative size and determine maximum heat rejection.

I. Introduction

Nuclear power systems for long-term Lunar and Martian missions present many challenges to thermal management systems, such as variable thermal loads, large temperature swings between day and night, and freezing of the working fluid. A Variable Conductance Heat Pipe (VCHP) radiator can passively accommodate the changing thermal load and environment conditions. In a VCHP, a non-condensable gas is added that blocks a portion of the condenser. The gas charge blocks more of the condenser as the heat pipe evaporator temperature is reduced. This variable thermal link allows the heat pipe evaporators (and any attached heat exchanger) to remain at an almost constant temperature during variations in power and heat sink conditions. In addition to passively controlling the thermal load, the gas allows the fluid in the heat pipe to freeze in a controlled fashion as the heat pipe is shut down, avoiding damage, and aids with start-up from a frozen condition.

NASA is currently considering Stirling power conversion systems for surface power applications with high-temperature heat-pipe radiators to reject the waste heat (Mason, Poston, and Qualls, 2008). A typical design showing the heat-pipe radiator panel assembly is shown in Figure 1. This type of modular design allows for the radiator panels to be compactly stowed during launch. During operation, waste heat from the Stirling convertors is removed by a pumped single-phase water loop. To reject the heat, the warm water passes through a series of heat

[1] Chief Engineer, AIAA Member, Bill.Anderson@1-act.com
[2] Sales Manager, Electronic Products
[3] R&D Engineer, Aerospace Products
[4] Manager, Aerospace Products, AIAA Member
[5] Vice President, Solar Power Systems, AIAA Member
[6] Principal Investigator, AIAA Member

exchangers with embedded heat pipes, which in turn are connected to the radiator panels. Since the heat pipes operate independently of one another, the system is inherently redundant and will continue to function effectively even if struck by micrometeoroid and orbital debris (MMOD). Studies have shown that a vertical radiator rejecting heat from both surfaces provides the highest efficiency. Orienting the radiator surfaces coplanar to the ecliptic provides the lowest maximum sink temperature at the equator (Dallas, Diaguila, and Saltsman, 1971). The vertical orientation (with respect to lunar gravity) also improves the performance of the embedded heat pipes. When the evaporator is placed at the lowest level, the heat pipe becomes completely gravity assisted and works as a thermosyphon. Unlike a heat pipe, a thermosyphon requires no wick in the condenser. Removal of the condenser wick provides the lowest possible liquid return pressure drop and allows the thermosyphon to transport more power than a fully-wicked heat pipe of similar geometry.

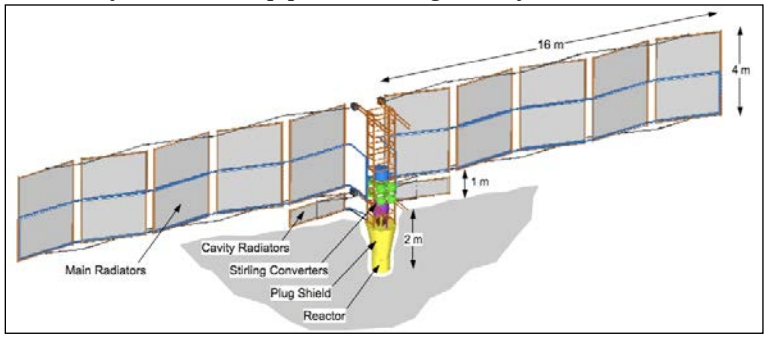

Figure 1. Fission Surface Power System Concept (Mason, Poston, and Qualls, 2008).

In a conventional heat pipe radiator, the heat pipes are totally passive and the radiator is sized to carry the highest power at the highest sink temperature. This radiator is then oversized for other conditions, such as the Lunar/Martian night, or periods when the power to be rejected is low. As the environment changes, the heat exchanger and heat pipe temperatures must be monitored. As sink temperature drops, the heat pipes dump more power and the reactor output must be controlled to keep the secondary loop and heat pipe temperatures constant. By substituting VCHPs for the heat pipes, the radiator will automatically adapt to changing conditions. Such a design eliminates the need for control of the reactor output to prevent freezing in the heat pipes. With VCHPs, freezing of the working fluid becomes permissible since the non-condensable gas adds freeze/thaw tolerance to the heat pipes.

II. VCHP Radiator Design

A. Requirements

Thermal requirements for the radiator are given in Table 1. The VCHP radiator needs to do the following:

1. Operate in the temperature range from 370 to 400 K.
2. Minimize mass.
3. Accommodate the Coefficient of Thermal Expansion (CTE) mismatch between the titanium heat exchanger and the Graphite Fiber Reinforced Composite (GFRC) panel face sheets.
4. Allow the heat pipes to continue to operate with minimum temperature drop as the power is reduced.
5. Startup with free water frozen in an arbitrary position during transit to the moon.
6. Survive multiple freeze/thaw cycles.

Table 1. System Thermal Specifications.

Radiator Thermal Power	70 kW_{th}
Radiator Outlet Temperature	370 K
Radiator Inlet Temperature	400 K
Individual Thermosyphon Power	≈500 W
Sink Temperature - Shackleton Crater	114 K to 212 K
Sink Temperature - Equator	101 K to 314 K
Condenser Length	2 m
Panel Emissivity	0.9

B. Previous Work

To date, all space radiators have used ammonia, ethane, or propylene as the working fluid, and have operated at temperatures below roughly 430 K, which is substantially below the required temperatures for the current system.

In previous work the authors reviewed suitable heat pipe working fluids, envelope materials, and radiator facesheets (Anderson and Stern, 2005, Stern and Anderson, 2005), and determined that a titanium/water heat pipe radiator with Graphite Fiber Reinforced Composite (GFRC) facesheets was suitable for this application. At that time, the long term compatibility of titanium/water heat pipes had not been demonstrated so a series of titanium/water heat pipe life tests were started. (Anderson et al., 2012, 2013). The titanium/water heat pipes are compatible at temperatures up to 550 K, based on ongoing life tests that have been running for up to 72,000 hours (8.2 years) as of May 2013. Analysis of titanium/water heat pipe cross-sections using optical and electron microscopy revealed little if any corrosion even when observed at high magnifications.

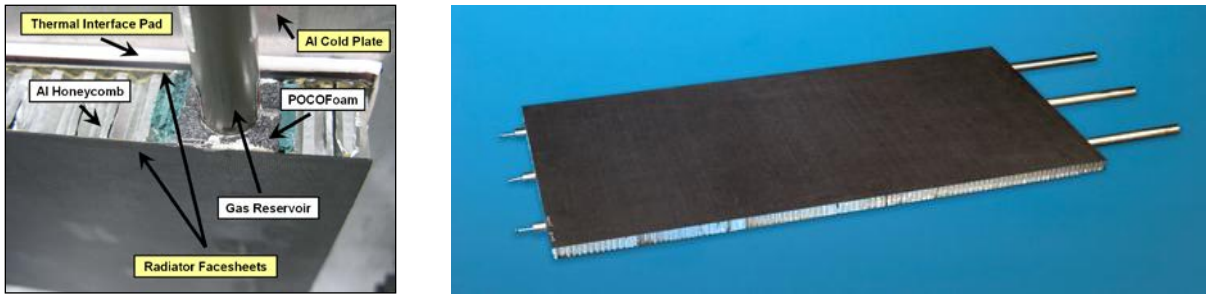

(a) **(b)**

Figure 2. (a) End view of radiator, showing components (b) Previous Radiator Demonstration Unit (RDU) panel did not constrain the heat pipe evaporators.

As shown in Figure 2(a), the previous radiator panels had the following:

1. A series of titanium/water heat pipes to transfer heat from the secondary fluid to the radiator panel
2. High conductivity foam saddles to form an interface between the circular heat pipe and the flat fin and accommodate the CTE mismatch
3. High conductivity GFRC fins
4. Aluminum honeycomb to provide stiffness to the structure

The previous Radiator Demonstration Unit (RDU) panel, shown in Figure 2(b), accommodated the CTE mismatch between the heat pipes and the facesheets by controlling the weave angle to match the CTE of the facesheet and panel along the heat pipe axis. The CTE mismatch perpendicular to the axis was accommodated by the compliance provided by the graphite foam saddles (Anderson, Sarraf, Garner, and Barth, 2006). It is important to note that the heat pipes in the previous radiator panel were not constrained from expanding in a direction perpendicular to the heat pipe axis.

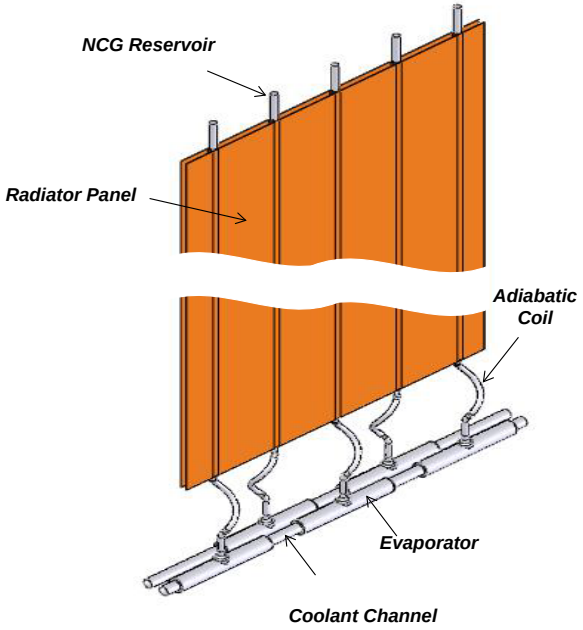

Figure 3. Radiator Panel and Titanium Heat Exchanger Schematic.

C. Radiator Panel Overview

A schematic of the final radiator panel and integrated titanium heat exchanger design is shown in Figure 3. This panel had a number of improvements from the previous RDU panel:

- Panel integrated with a titanium heat exchanger
- Annular heat pipe evaporator to minimize mass
- Coiled adiabatic section to accommodate the C.T.E. mismatch
- Wick design to allow the heat pipe to operate when tilted, and to start-up from a frozen state when the excess water is frozen in an arbitrary position.

III. Titanium Heat Exchanger Interface Trade Study

Three different concepts were evaluated for the heat exchanger between the coolant lines and the VCHP radiator. Design considerations include ease of fabrication, modularity and redundancy potential, heat transfer performance, mass, and failure risk reduction. The primary selection criterion is specific power, the system's ability to radiate the waste heat with the lowest possible mass. As shown in Figure 4, the three designs considered were:

1. Graphite foam saddle between the coolant channel and the heat pipe.
2. Bent tube inserted into the coolant channel
3. Annular evaporator over coolant channel

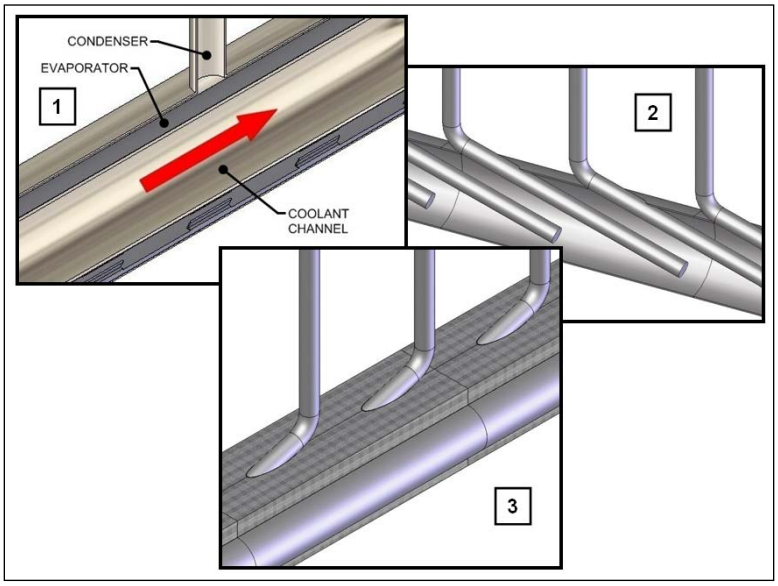

Figure 4. Heat Exchanger Designs: 1 – Annular, 2 – Bent Tubes, 3 – POCO Foam Saddle.

The heat exchanger/heat pipe radiator specific power was calculated using the method developed by Anderson and Stern (2005). For each of the three interfaces, the trade study varied a number of relevant parameters to determine the minimum mass. For example, the Fin Width (Heat Pipe Spacing), Evaporator Length, and Condenser Diameter were varied for the annular evaporator design. Details of the calculations are given in Anderson, Muzyka, and Hartenstine (2013).

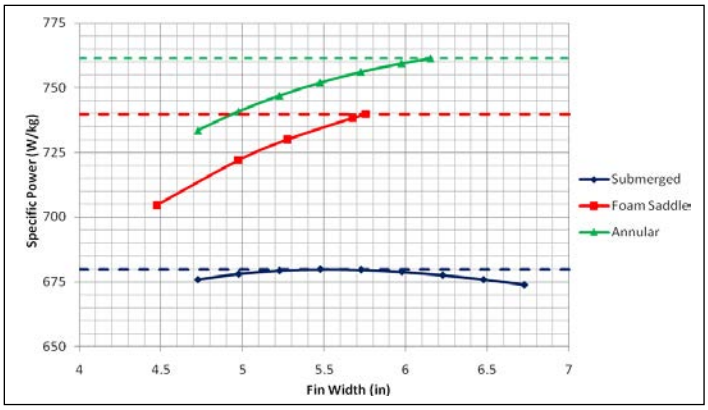

Figure 5. Comparison of Optimized Designs for Each Interface (Shackleton Crater).

In the annular evaporator concept, shown in Figure 4(1), the VCHP evaporator surrounds the coolant flow. If the evaporators cover the entire available length, then this concept offers some MMOD protection, since the outer wall and screen wicks will "bumper" the impact. In addition, this design offers the largest evaporator heat transfer

surface area of the three concepts. Since there will be two coolant loops; every second annular evaporator will be attached to each coolant loop; see Figure 3. This allows the evaporator to be twice as long as the spacing between heat pipes.

The optimized specific power as a function of fin width for the 3 interfaces is compared in Figure 5. Due to the small temperature drop from the coolant channel to the vapor, the annular evaporator offers the most benefits. It is a fairly simple design for assembly; it requires the fewest heat pipes to dissipate the total input power, and has the lowest mass for the overall design. For optimized designs the annular evaporator has 3.8 % greater specific power than the foam saddle design, and 13 % greater specific power than the submerged evaporator design.

IV. Adiabatic Section Design and CTE Mismatch

An important part of the radiator design was accommodating the CTE mismatch between the titanium heat pipes and heat exchangers, versus the GFRC facesheets. Titanium has a CTE of about 8.6 μm/m °C, while the GFRC facesheets have different CTEs in orthogonal directions. In the RDU, the facesheet layup was chosen so that the GFRC CTE was matched to the titanium CTE along the axis of the heat pipe. The heat pipes were allowed to float in the direction perpendicular to the heat pipe axis.

By adding the titanium heat pipe heat exchanger as shown in Figure 3, stresses occur whenever the temperature of the system is different from the bonding temperature. Because matching the CTE in the longitudinal (y) direction, the CTE in the lateral (x) direction to is negative. This means that as the temperature is increased, the titanium heat exchanger grows, in the x direction, while the facesheet shrinks, see Figure 6.

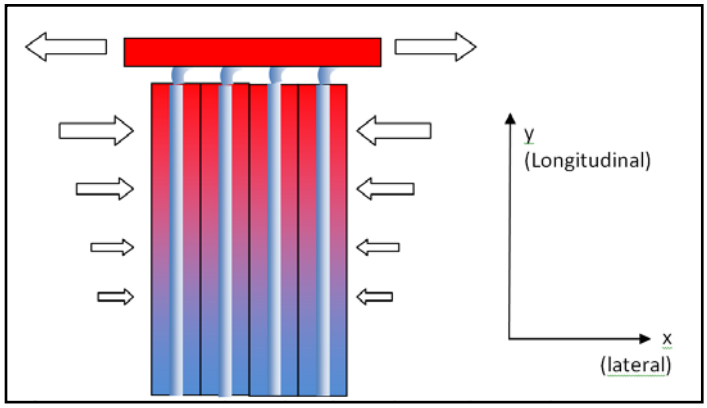

Figure 6. Differential CTE from Temperature Gradients along the Condenser Tubes.

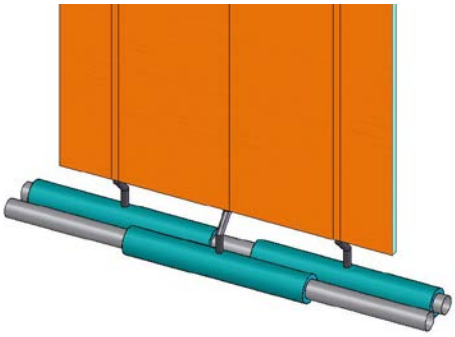

Figure 7. The stresses were too high in the original concept, where the adiabatic section was bent between the evaporator and the condenser.

In the initial radiator concept, the CTE mismatch was to be accommodated by the bending the adiabatic section between the top of the evaporator and the heat pipe condensers; see Figure 7. Stress analysis showed that the stresses in the titanium adiabatic section were too high, so other designs were examined. The constraints were:

- The bend should not extend past the coolant channel to allow the system to fold up.
- The top of the condenser is displaced 0.875 inches (2.22 cm) from the bottom to align with both the coolant channel on bottom and the radiator panel on top.

The revised concept is shown in Figure 8, where helical condenser coils provide compliance. FEM analysis showed that this reduced the maximum stress to less than one-quarter of the yield stress, providing an acceptable design.

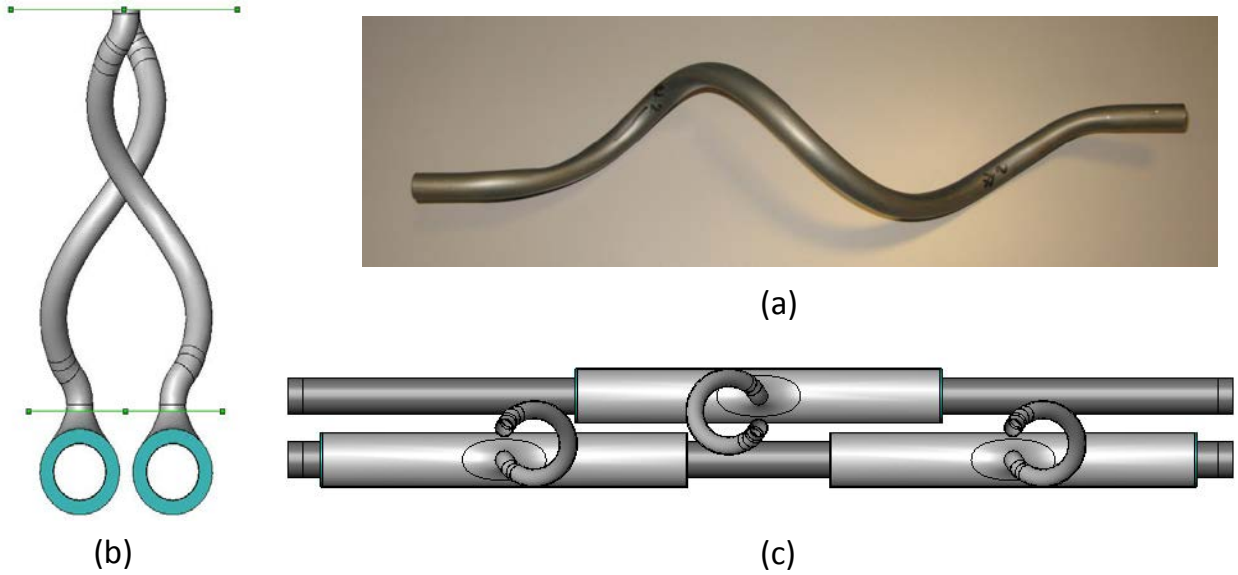

Figure 8. (a) Helical Condenser Coils to Add Flexibility to the Heat Exchanger. (b) Coils are parallel at the top and bottom planes and align in the center to meet the radiator panel. (c) Top-down view showing how the coils line up in a plane for the heat pipe condensers.

An FEM model was used to determine the maximum displacement the heat exchanger could handle while maintaining a factor of safety (FOS) of 4 or above. Figure 9 shows the FOS distribution, which also corresponds to the stresses. As the radiator panel increases in width, the displacement of the titanium heat exchanger also increases. The stresses shown in Figure 9 correspond to a design with 11 VCHPs in a panel.

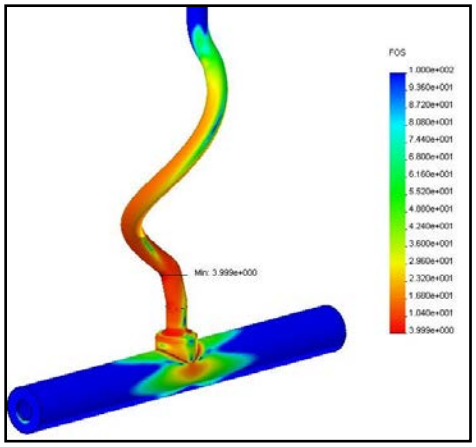

Figure 9. FEA Model Showing Factor of Safety for a design with 11 VCHPs in a single panel.

V. Wick Design and Freeze/Thaw Tolerance

D. Wick Design for Tilt

Since the moon is not completely flat, the radiator on the lunar surface could be tilted at up to 5°. Therefore it is vital that the VCHP be able to start up and operate at slight angles. To do this, the wick needs to be capable of

overcoming the gravitational, liquid, and vapor pressure drops of the system, where gravitational pressure accounts for over 90 % of the total pressure drop. Figure 10 shows the evaporator in a tilted orientation.

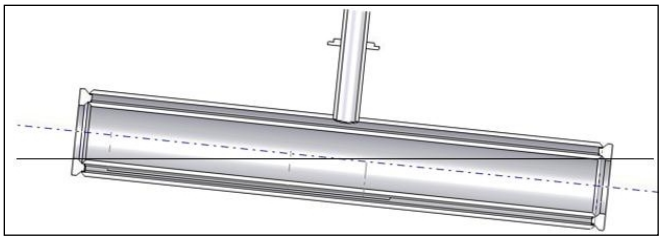

Figure 10. Evaporator with a Titled Orientation.

A screen wick is used in the condenser, with the mesh was sized so that liquid could return from the lowest point on the heat pipe evaporator to the highest part of the inner cylinder, to insure that the entire wick was saturated. The evaporator design can experience any tilt angle on the moon and can pump against a 2° tilt angle on earth.

E. Non-Condensable Gas Improves Freeze/Thaw Tolerance

The addition of NCG allows a thermosyphon to more easily start after freezing. When power is reduced in a Constant Conductance Heat Pipe (CCHP), vapor will continue to flow from the evaporator to the colder condenser region. There the vapor would freeze, and eventually the evaporator region would dry out. A VCHP, however, benefits from the presence of non-condensable gas during the freezing process. As temperature drops and approaches the freezing temperature in the condenser, the vapor pressure within the VCHP decreases. The non-condensable gas expands to maintain pressure equilibrium at the vapor-gas interface, reducing the active condenser length in the process. This has the effect of both restricting the flow of vapor to the inactive portion of the condenser and maintaining the active condenser section at a higher temperature than an equivalent CCHP at the same power level. As the working fluid temperature reaches a limit specified by design, the entire condenser section is occupied by non-condensable gas. Further decrease in temperature beyond this shutoff point will result in the gas expanding into the adiabatic section. When freezing occurs, the working fluid is restricted to the evaporator and adiabatic regions.

Ochterbeck and Peterson (1993) found ice to form in the condenser as a concentrated deposit rather than evenly distributed along the condenser length when testing in a horizontal orientation. Over time, this deposit grew inward, in some cases blocking the condenser from the evaporator. These researchers found that for larger non-condensable gas charges, blockage did not occur. Furthermore, for heat pipes with a large condenser to evaporator ratio, such as those designed for the Lunar VCHP Radiator, blockage should not occur

A previous paper demonstrated the ability of a VCHP thermosyphon to restart after freezing, with frozen conditions maintained up to 15 days (Ellis and Anderson, 2009). In these tests, the VCHP was upright and exposed to expected sink temperatures, with power turned down or shut off. The VCHP was a simple bent pipe design with a 0.375 inch (0.95 cm) inside diameter. There were several freeze angles that produced startup failure. These results showed that the VCHP could be successfully frozen and restarted in a gravity field, but freezing of the liquid in an arbitrary position during transit was still a concern.

This work has been extended in this paper by examining freeze/thaw performance outside of normal operating conditions. In particular, the VCHP can freeze during the zero-g transit to the moon. In this case, there is no defined gas/vapor interface and the NCG will not keep working fluid in the evaporator. Any water not contained in the wick can freeze in an arbitrary location in the heat pipe (Jaworske, Sanzi, and Siamidis, 2008). This water will not be available to start the heat pipe on the moon, and can make restart difficult.

VI. Freeze/Thaw Testing

F. Annular Evaporator Freezing Positions

A VCHP with an annular evaporator was fabricated for freeze/thaw testing. A cylindrical heater block was inserted into the inside of the annulus to provide heat during testing. An adjustable height work stand with a rotating arm is used to hold the VCHP during testing. The rotating arm allows the VCHP to be moved from the adverse freezing position to the intended operating position while coolant continues to run through the cooling jacket. The

coolant is supplied to the calorimeter by a rotary vane pump connected to a ten gallon supply tank. The supply tank contained 50/50 ethylene glycol-water mixture cooled by liquid nitrogen.

Since the purpose of this experiment is to show that the VCHP can hold the fluid at any freeze orientation, a number of different angles were tested (Table 2). The condenser angles and evaporator angles are shown schematically in Figure 11.

Table 2. Freezing Orientations.

Test Run	Condenser Angle	Evaporator Angle
1. Normal Operating Position	90°	-
2. Slightly Gravity Aided	10°	0°
3. Horizontal	0°	0°
4. Slightly Against Gravity	-10°	0°
5. Half Against Gravity	-45°	0°
6. Upside Down	-90°	-
7. Rotated Horizontally	0°	90°
8. Rotated Slightly Horizontally	0°	10°
9. Rotated Half Horizontally	0°	45°
10. Combination	-10°	10°
11. Combination 2	-45°	45°

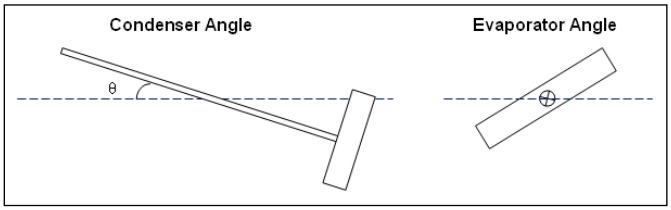

Figure 11. Testing Angles.

G. Annular Evaporator Freeze/Thaw Temperature Profiles

If the wick contains enough fluid in all orientations, then the orientation in which the VCHP is frozen in will not affect startup. When the VCHP is operating correctly, the pressure in the VCHP should allow the vapor to start pushing the NCG back up into the condenser at a temperature around 30 °C. Before this time, the thermocouples on the evaporator should see a gradual rise while the thermocouples on the condenser stay frozen. Once the vapor pressure is high enough, the NCG front will gradually retreat, and the thermocouples on the condenser will begin to increase to vapor temperature one by one as the front passes. Vapor temperature and evaporator temperature will continue to rise gradually during this process until equilibrium is reached.

During testing, the VCHP was frozen for a duration of one hour in the specified orientation; see Table 2. The VCHP was then rotated back to normal operating position before receiving input power. No problems were observed during startup. Shown in Figure 12 is the temperature profile of the worst case scenario (frozen at -90°). Note that the plot indicates a successful startup of the heat pipe.

Since the heat pipe could start up in all orientations, it was apparent that the wick retained enough liquid. To make sure no liquid was simply getting hung-up in the annular design instead of the wick, the VCHP was drained by tilting the condenser to -80° and -110° for 15 minutes a side while in the thawed state. Then the VCHP was frozen at -90° for one hour. After rotating to the operating orientation and applying power, the VCHP successfully started up and had a temperature profile similar to Figure 12. This set of tests indicates that the annular heat pipe design can be successfully started up with the liquid frozen in any location.

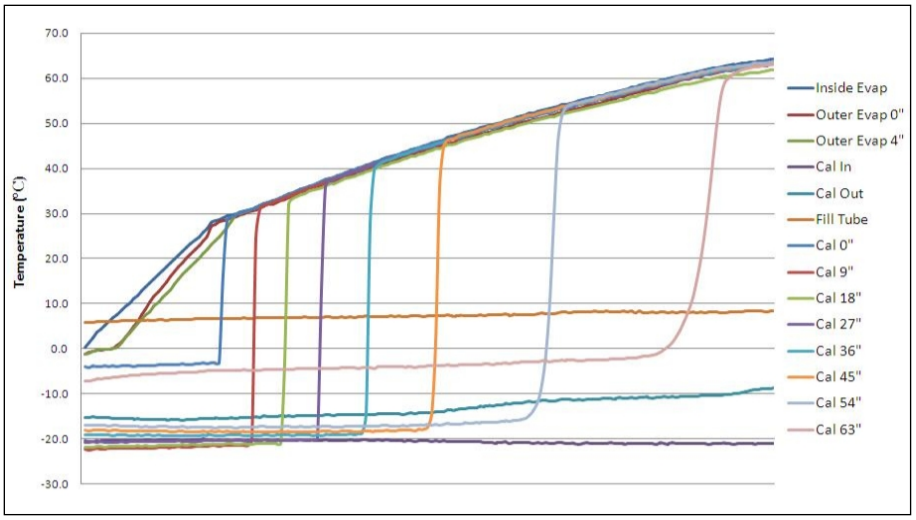

Figure 12. Temperature Profile When VCHP Was Frozen -90° from Horizontal.

H. Annular Evaporator Long Duration Freeze Test

In addition to the short term tests described above, a long duration freeze test was also conducted to simulate the conditions the VCHP will experience in lunar transit, and during the 15-day-long lunar night. To do this the VCHP was drained as discussed above and was then held frozen for 15 days at -90°. After 15 days the VCHP was placed at normal operating position and power was supplied to the evaporator. The temperature profile shown in Figure 13 indicates sufficient fluid was stored in the evaporator wicks and startup was successful.

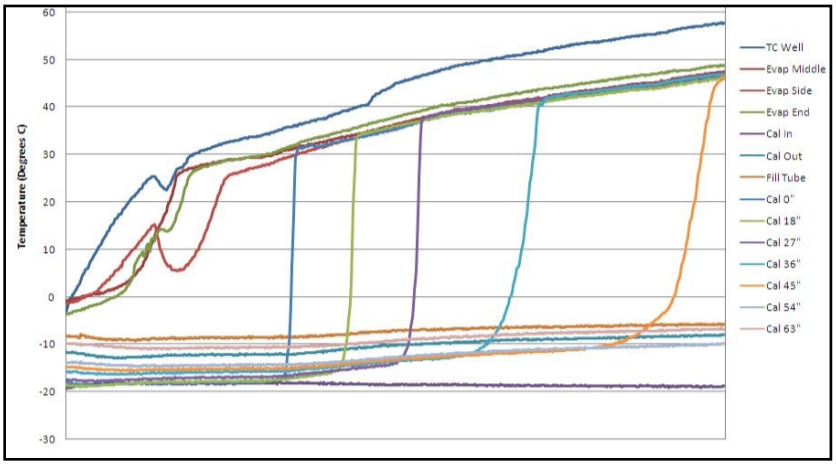

Figure 13. Temperature Profile of VCHP Startup after 15 Day Freeze.

The anomalies in the evaporator at the beginning of startup simply show the fluid melting and pieces of ice falling down to cause a non-uniform temperature profile, however once vapor began to form the VCHP acquired its normal profile.

VII. Full Length VCHP Radiator Panel Fabrication

A full-length (2 meter tall overall) radiator panel was fabricated, based on the concept shown in Figure 3. The dimensions of the system are shown in Table 3. A picture of the VCHP radiator panel and titanium heat exchanger is shown in Figure 14, while Figure 15 shows a detail of the top of the radiator. The reservoirs are a continuation of the condenser, located above the radiators. To maximize the radiator panel length the condensers were angled. The angle was chosen at 30° to allow fluid to drain with gravity but still save room for greater panel length.

Table 3. System Final Dimensions.

Variable	Dimension
Coolant Channel Outer Diameter	0.5 in (1.27 cm)
Coolant Channel Wall Thickness	0.035 in (0.089 cm)
Evaporator Outer Diameter	1.125 in (2.86 cm)
Evaporator Wall Thickness	0.035 in (0.051 cm)
Evaporator Length	10 in (0.254 m)
Condenser Outer Diameter	0.5 in (0.953 cm)
Condenser Wall Thickness	0.035 in (0.089 cm)
Condenser Length (inside radiator facesheet)	66.9 in (170 cm)
Condenser Helical Coil Length	≈7 in (17.8 cm)
Primary Wick (welded around coolant channel)	3 Wraps, 100 Mesh
POCO Saddle Minimum Thickness	0.113 in (0.287 cm)
Radiator Facesheet Thickness	0.012 in (0.030 cm)
Heat Pipe Spacing	6.8 in (17.27 cm)
Working Fluid	Water
Non-Condensable Gas	Helium

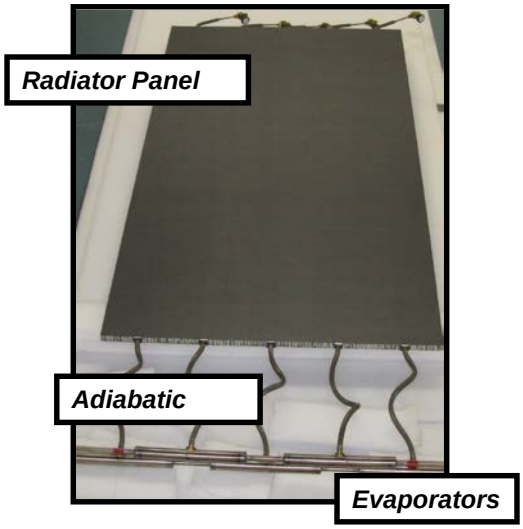

Figure 14. Radiator Panel with 170 cm condensers.

Spacecraft VCHPs are generally use argon as the non-condensable gas. Helium was selected for these VCHPs, because they are designed to operate in a gravity field, on both the Earth and Moon. It was chosen because it would be less dense than the water vapor, and would tend to rise to the reservoir and end of the condenser. The gas-charge was chosen so that the condenser would be completely blocked around 300 K.

Radiator Panel Testing

A. Test Set-up

Because extensive thermal-vacuum tests were planned at NASA GRC, only a cursory set of tests were conducted on the program to demonstrate operation at nominal powers and temperatures, and shutdown at temperatures around 300 K. The finished VCHP radiator system (with radiator panel and embedded VCHPs) is shown in Figure 16. The radiator is tested in an upright orientation, and supported by aluminum stands. It is also fully instrumented with TCs (red dots). The panel was upright which allows the VCHPs to operate in thermosyphon mode (i.e., reflux mode), which is what would occur on the Lunar Surface.

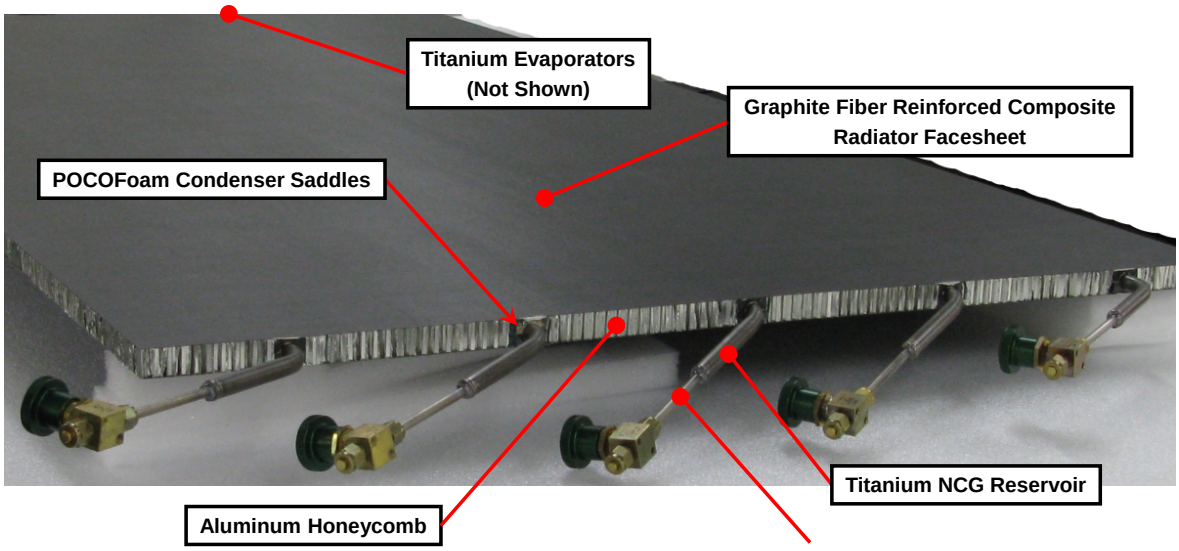

Figure 15. End-View Showing the VCHP Reservoirs, the POCO foam saddles, and the aluminum honeycomb.

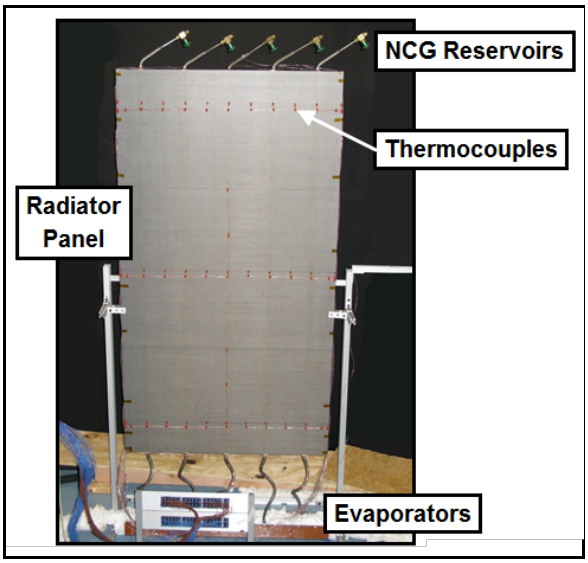

Figure 16. Full-Scale VCHP Radiator in Testing Configuration.

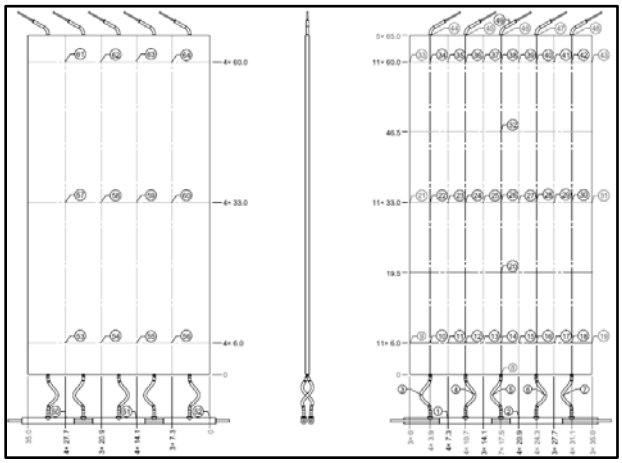

Figure 17. Map of TC Locations.

A map of the thermocouple locations is shown in Figure 17. There were 67 TCs in all. TC65, TC66 and TC67 measured the temperature of the coolant inlet, coolant outlet and ambient, respectively. Recording the coolant inlet and outlet temperatures allowed flow calorimetry to be performed to determine the total heat rejection capability of the radiator system. The centermost VCHP was more heavily instrumented with TCs than the other VCHPs to track the movement of the vapor/gas front during shutdown.

During these preliminary tests, the radiator was not placed in a vacuum chamber, but rather tested in the ambient. This increases the heat rejection rate since natural convection will occur in addition to radiation, giving a higher heat rejection rate without requiring a cold wall. Hot water is supplied to the titanium heat exchanger using a Sterling temperature control unit to pump water at the radiator operating temperature of 400 K (127 °C).

Testing at ACT consisted of: 1) Determining the maximum heat rejection rate of the system and 2) Demonstrating successful shutdown of the VCHPs when the inlet coolant temperature was lowered. The radiator panel was shipped to NASA GRC for extensive thermal-vacuum testing.

B. Full-Scale Radiator Testing – Nominal Operation (120 °C)

Testing at ACT consisted of steady-state operation at the nominal operating temperature, followed by operation at lower temperatures to demonstrate radiator shutdown. Figure 18 shows a plot of the steady-state temperatures of the radiating surface during nominal operation. The condensing sections of the embedded VCHPs are indicated by the linear higher temperature regions. Overall, the panel shows good isothermality with a ΔT of 26 °C from the centermost VCHP condenser to one of its symmetry planes.

The temperature of each evaporator was raised to 120 °C to bring the entire panel into nominal operation. The ambient temperature in the laboratory was a constant 23 °C. Figure 18 shows a plot of the steady-state temperatures of the radiating surface. Note that this plot was generated by interpolating the data from 33 discrete temperature readings (see Figure 17 for specific locations). The condensing sections of the embedded VCHPs are indicated by the linear hotspots. The radiator surface temperature decreases when traveling away from the condensers to the symmetry planes. The symmetry planes are located midway between each set of VCHP condensers and are perpendicular to the radiating surface. The surface temperatures reach their minimum values at these symmetry planes. Overall, the panel shows good isothermality with a ΔT of 26 °C for the centermost VCHP condenser to one of its symmetry planes.

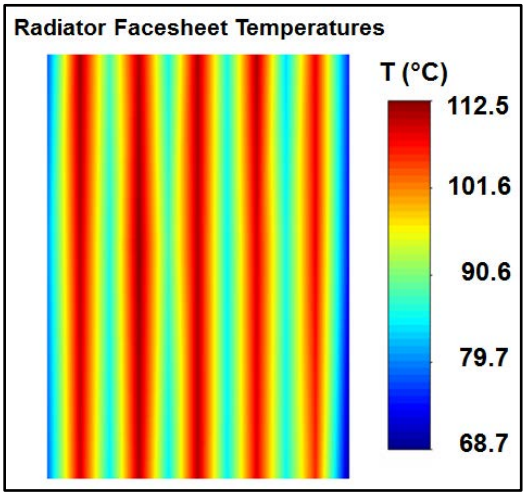

Figure 18. Thermal Profile of Radiating Surface for Full-Scale Panel (120 °C Nominal).

Table 4 lists the numerical results of the panel during nominal operation. The entire panel is capable of transporting 3.8 kW, which corresponds to 760 W per heat pipe.

Table 4. Numerical Results for 120 °C Nominal Operation.

	ΔT (°C)	Q (kW)
Evaporator to Condenser	3	-
Condenser to Facesheet	4	-
Across Radiator Facesheet (Center VCHP)	26	-
Total Rejected Power	-	3.8

Figure 19 shows the temperature profile of the centermost VCHP. The temperature is maximum at the evaporator and minimum at the gas reservoir. The temperature is lowest at the gas reservoir because non-condensable gas blocks the flow working fluid vapor to this portion of the heat pipe, as desired. In general, the heat pipe is isothermal with an evaporator to condenser ΔT of 3 °C. Table 4 lists the numerical results for the panel during nominal operation. The entire panel is capable of transporting 3.8 kW, which corresponds to 760 W per heat pipe.

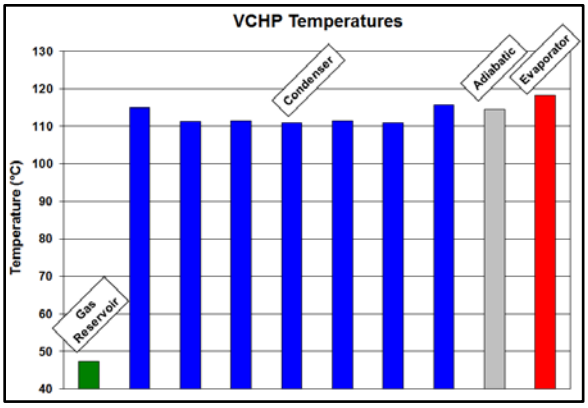

Figure 19. Thermal Profile of Center VCHP for Full-Scale Panel (120 °C Nominal).

C. Full-Scale Radiator Testing – VCHP Shutdown (35 °C)

The temperature of each evaporator was lowered to 35 °C to allow the non-condensable gas to expand into the condenser and cause the VCHPs in the panel to shut down. This state of shutdown is evident in Figure 20 and Figure 21. Note that the panel is roughly isothermal and has equilibrated to the temperature of the ambient. There is an evaporator-to-condenser ΔT of 12 °C since non-condensable gas has filled all of the condenser and adiabatic section and blocks the flow of vapor to these portions of the heat pipe. The numerical results of this test are tabulated in Table 5. The panel rejects minimal power during shutdown.

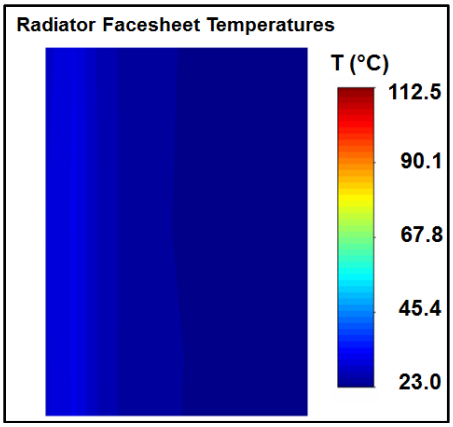

Figure 20. Thermal Profile of Radiating Surface for Full-Scale Panel (35 °C Shutdown).

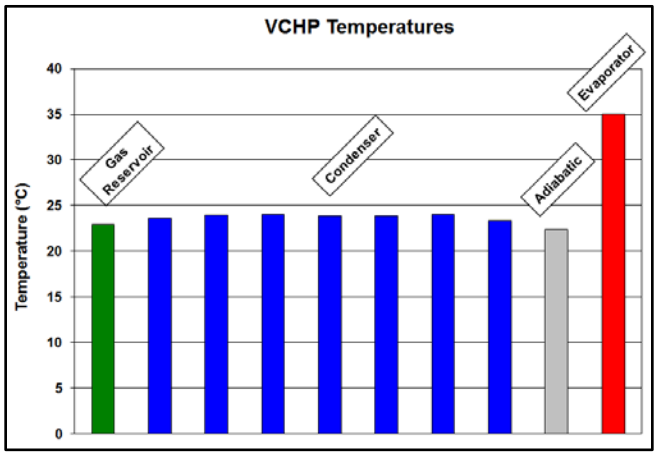

Figure 21. Thermal Profile of Center VCHP for Full-Scale Panel (35 °C Shutdown).

Table 5. Numerical Results for 35 °C Shutdown.

	ΔT (°C)	Q (kW)
Evaporator to Condenser	12	-
Condenser to Facesheet	< 1	-
Across Radiator Facesheet (Center VCHP)	< 1	-
Total Rejected Power	-	0

D. Thermal-Vacuum Chamber Testing – NASA GRC

After the minimal testing discussed above, the VCHP was extensively tested at NASA GRC in a large thermal vacuum chamber. A series of tests measured the radiated power from the panel as a function of water inlet temperature and flow rate. In a second test, the heat exchanger manifold was drained of water, and then the system was exposed to cold temperatures to freeze it. The system was successfully restarted after it was frozen. Details are given in Jaworske, Gibson, and Hervol (2012).

VIII. Conclusion

Nuclear power systems for long-term Lunar and Martian missions present many challenges to thermal management systems, such as variable thermal loads, large temperature swings between day and night, and freezing of the working fluid. The radiator to reject the waste heat must be sized for the maximum power at the highest sink temperature, but is then oversized for other conditions, such as the Lunar/Martian night, or periods when the power to be rejected is low. A Variable Conductance Heat Pipe (VCHP) radiator can passively accommodate changing thermal loads and environments. The VCHP radiator needs to do the following:

- Operate in the temperature range from 370 to 400 K.
- Low mass.
- Accommodate the Coefficient of Thermal Expansion (CTE) mismatch between the titanium heat exchanger and the Graphite Fiber Reinforced Composite (GFRC) panel face sheets.
- Allow the heat pipes to continue to operate with minimum temperature drop as the power is reduced.
- Startup with free water frozen in an arbitrary position during transit to the moon.
- Survive multiple freeze/thaw cycles.

A panel was designed with a number of improvements over previous Lunar radiator panels:

- Panel integrated with a titanium heat exchanger
- Annular heat pipe evaporator to minimize mass
- Coiled adiabatic section to accommodate the C.T.E. mismatch
- Wick design to allow the heat pipe to operate when tilted, and to start-up from a frozen state when the excess water is frozen in an arbitrary position.

Freeze/thaw testing was conducted on a single heat pipe with an annular evaporator. These tests demonstrated start-up after short term freezing in a number of arbitrary positions. A final freeze/thaw test showed that the VCHP started up after remaining frozen for fourteen days, the length of a Lunar night.

A full length VCHP radiator panel was fabricated with five heat pipes, and then tested for nominal operation and VCHP shutdown. During nominal operation, the panel ran at 120°C (evaporator temperature) and total power rejection was measured via flow calorimetry. The panel was able to transport 3.8 kW. Thermocouple readings indicated that the radiating surface possessed good isothermality ($\Delta T \approx 26$ °C). For the shutdown demonstration, the evaporator temperature was lowered to 35 °C to allow the non-condensable gas to expand into the condenser and adiabatic section, causing the heat pipes to shut down. During shutdown, the system stopped rejecting heat to the environment and the radiator surface equilibrated to the ambient temperature. Thermal vacuum testing at NASA GRC demonstrated the ability of the system to restart after the heat pipes were frozen.

Acknowledgments

This research was sponsored by NASA Glenn Research Center under Contract No. NNX09CA43C. Mr. Lee Mason of NASA Glenn was the technical monitor. We would also like to thank Don Jaworske, Jim Sanzi, and John Siamidis for helpful discussions on high temperature radiators. Rodney McClellan and Dennis Palm served as the technicians on the project. This Phase II program expanded upon the SBIR Phase I work completed by Kara Walker and Michael Ellis. Any opinions, findings, and conclusions or recommendations expressed in this article are those of the authors and do not necessarily reflect the views of the National Aeronautics and Space Administration.

References

W. G. Anderson and T. Stern, "Heat Pipe Radiator Trade Study for the 300-550 K Temperature Range," STAIF 2005, Vol. 746, pp. 187-194, Albuquerque, NM, February 13-17, 2005.

W. G. Anderson, D. B. Sarraf, S. D. Garner, and J. Barth "High Temperature Water-Titanium Heat Pipe Radiator,", Proceedings of the 2006 IECEC, ISBN-10: 1-56347-800-5, AIAA, San Diego, CA, June 26-29, 2006. http://www.1-act.com/wp-content/uploads/2013/01/IECEC-2006-High-Temperature-Water-Titanium-Heat-Pipe-Radiator.pdf

W. G. Anderson, S. Tamanna, C. Tarau, J. R. Hartenstine, and D. L. Ellis, "Intermediate Temperature Heat Pipe Life Tests", 16th International Heat Pipe Conference, Lyon, France, May 20-24, 2012. http://www.1-act.com/wp-content/uploads/2013/03/010-16ihpc-Anderson-Intermediate-Temperature-Heat-Pipe-Life-Tests-Rev-6.pdf

William G. Anderson, Bryan J. Muzyka, and John R. Hartenstine, "Variable Conductance Heat Pipe Radiator Trade Study for Lunar Fission Power Systems," Nuclear and Emerging Technologies for Space (NETS-2013), Albuquerque, NM, February 25-28, 2013. http://www.1-act.com/wp-content/uploads/2013/03/NETS2013-VCHP-Radiator-Trade-Study-for-Lunar-Fission-Power-Systems-Final.pdf

W. G. Anderson, S. Tamanna, C. Tarau, J. R. Hartenstine, and D. Ellis, "Intermediate Temperature Heat Pipe Life Tests and Analyses," 43rd International Conference on Environmental Systems (ICES 2013), Vail, CO, July 14-18, 2013.

M. C. Ellis and W. G. Anderson, "Variable Conductance Heat Pipe Performance after Extended Periods of Freezing," Space, Propulsion and Energy Sciences International Forum (SPESIF 2009), Huntsville, AL, February 24 - 27, 2009. http://www.1-act.com/wp-content/uploads/2013/01/SPESIF-2009-VCHP-Heat-Pipe-Performance-after-Extended-Periods-of-Freezing.pdf

D. A. Jaworske, J. L. Sanzi, and J. Siamidis, "Cold Start of a Radiator Equipped with Titanium-Water Heat Pipes", 6th Annual IECEC, Cleveland, OH, July 29-31, 2008.

D. A. Jaworske, M. A. Gibson, and D. S. Hervol, "Heat Rejection from a Variable Conductance Heat Pipe Radiator Panel," Nuclear and Emerging Technologies for Space (NETS-2012), The Woodlands, TX, March 21-23, 2012. http://ntrs.nasa.gov/archive/nasa/casi.ntrs.nasa.gov/20120004033_2012004257.pdf

T. Dallas, A.J. Diaguila, and J.F. Saltsman, "Design Studies on the Effects of Orientation, Lunation, and Location on the Performance of Lunar Radiators", NASA Technical Memorandum 1846 (1971).

L. Mason, D. Poston, and L. Qualls, "System Concepts for Affordable Fission Surface Power", NASA Technical Memorandum 215166 (2008).

J. M. Ochterbeck and G. P. Peterson, "Freeze/Thaw Characteristics of a Copper/Water Heat Pipe: Effects of Noncondensible Gas Charge," J. Thermophysics and Heat Transfer, 7, 1, (1993).

T. Stern and W. G. Anderson, "High Temperature Lightweight Heat Pipe Panel Technology Development," Proceedings of the Space Nuclear Conference 2005, pp. 198-202, San Diego, California, June 5-9, 2005. http://www.1-act.com/wp-content/uploads/2013/01/Space-Nuclear-Conference-2005-High-Temperature-Lightweight-Heat-Pipe-Panel-Technology-Development.pdf